

Received: 2020.03.01
Accepted: 2020.05.21
Available online: 2020.06.10
Published: 2020.08.05

Integrated Analysis of Hub Genes and Pathways In Esophageal Carcinoma Based on NCBI's Gene Expression Omnibus (GEO) Database: A Bioinformatics Analysis

Authors' Contribution:
Study Design A
Data Collection B
Statistical Analysis C
Data Interpretation D
Manuscript Preparation E
Literature Search F
Funds Collection G

ACE **Tan Yu-jing**
C **Tang Wen-jing**
AEG **Tang Biao**

Department of Physiology, Hunan University of Chinese Medicine, Changsha, Hunan, P.R. China

Corresponding Author:
Source of support:

Tang Biao, e-mail: biaotang@hnuocm.edu.cn

Scientific Research Fund of Hunan Provincial Education Department (No. 19B436); Hunan Provincial Innovation Foundation For Postgraduates (No. CX2018B515); Open Fund of the Domestic First-Class Discipline Construction Project of Integrated Traditional Chinese and Western Medicine of Hunan University of Chinese Medicine (No. 2018ZXYJH35); First-Class Discipline Construction Project of Basic Medicine in 13th Five-Year Plan of Hunan University of Chinese Medicine (06)

Background:

Esophageal carcinoma (ESCA) is a health challenge with poor prognosis and limited treatment options. Our aim is to screen for hub genes and pathways associated with ESCA pathology as diagnostic or therapeutic targets.

Material/Methods:

We downloaded 2 ESCA-related datasets from the Gene Expression Omnibus (GEO) database. Subsequently, differentially expressed genes (DEGs) of ESCA were determined by statistical analysis. Both Gene Ontology (GO) and Kyoto Encyclopedia of Genes and Genomes (KEGG) pathway enrichment analysis of DEGs were performed using online analytic tools. Network analysis was employed to construct a protein-protein interaction (PPI) network and to filter hub genes. We evaluated the expression level and impact of hub genes on survival of ESCA patients using the OncoLoc webserver.

Results:

A total of 210 DEGs were identified. The GO analysis showed that the DEGs were enriched in cell division. The KEGG pathway analysis showed DEGs that were enriched in cell cycle regulation, known cancer pathways, the PI3K-Akt signaling pathway, and the cGMP-PKG signaling pathway. The top 10 hub genes were markedly upregulated in ESCA tissue compared with normal esophageal tissue. Moreover, the expression level of the hub genes was different at different pathological stages of ESCA. Further prognostic analysis identified that the top 10 hub genes were related to late survival of ESCA patients, while exhibiting few associations with early survival time.

Conclusions:


The signaling pathways involving the DEGs probably represent the pathological mechanism underlying ESCA. The hub genes were associated with survival of ESCA patients, and as such have the potential to serve as diagnostic indicators and therapeutic targets.

MeSH Keywords:

Computational Biology • Esophageal Neoplasms • Gene Expression

Full-text PDF:

<https://www.medscimonit.com/abstract/index/idArt/923934>

 3712

 3

 11

 61



Background

Esophageal carcinoma (ESCA) is the eighth most common cancer and the sixth most common cancer leading to death, with more than 456 000 sufferers worldwide [1,2]. Previous studies have documented that the overall 5-year survival of ESCA patients is approximately 15% to 25% [2].

ESCA includes two major subtypes: esophageal squamous cell carcinoma (ESCC), the predominant form, and esophageal adenocarcinoma (EAC), which affects a growing percentile of patients [3]. There are distinct differences between the pathological risks underlying these histological subtypes that affect their incidence. The mechanism underlying ESCC is complicated and embraces a broad spectrum of hazards contributing to its rapidly increasing incidence. There are two primary types of risk factors: inheritable and environmental factors. There are several environmental risks, including alcohol and tobacco consumption, low vegetable and fruit intake, and low socioeconomic status [4]. As for EAC, almost all cases are complicated by precancerous lesions called Barrett's oesophagus, which mainly derive from gastroesophageal reflux disease, a common condition throughout the human population [5]. Despite this, the risk of progression from this kind of chronic premalignant condition into EAC is low; approximately 0.12%, which makes it difficult to perform predictions of EAC from Barrett's oesophagus. Fortunately, there are some mechanistic connections between heritable elements and EAC. A meta-analysis demonstrated that single nucleotide polymorphisms (SNPs) located in the LPA, TPPP, and CEP72 genes were associated with high risk of both EAC and its premalignant precursor. SNPs near HTR3C and ABCC5 implicated this region as a specific locus for EAC [6].

Given its extremely invasive nature and poor prognosis among gastrointestinal malignancies, a majority of people die from ESCA, placing a heavy burden on the international economy [7]. When it comes to treatment, ESCA demands multidisciplinary knowledge, covering endoscopic procedures, neoadjuvant therapy with chemotherapy, chemoradiotherapy, surgery, and other procedures [8]. If early-stage, mild symptoms are neglected by patients and clinical workers, treatment will be even more difficult. Studies have demonstrated that early diagnosis of dysplasia allows for decisive therapy and ultimately lengthens survival time [9]. In addition, immuno-oncology therapies with molecular targets have emerged, promising early results among ESCA patients [10]. Pursuit of available biomarkers therefore has the potential to exert positive effects via early diagnosis and treatment.

At present, exploring pathological mechanisms of diseases based on bioinformatics theories has becoming an increasingly important and effective method [11]. With bioinformatics

analysis, researchers can gain comprehensive knowledge regarding the studied diseases from molecular data. More crucially, it can provide novel insight leading to early diagnosis, definitive treatment, and survival prediction [12]. Previous research in the bioinformatics field has yielded some achievements in ESCA knowledge, such as identification of associated genes and pathways and altered methylation associated with ESCA pathology [13,14]. However, analytical ability for ESCA has been limited due to insufficient sample size and a lack of in-depth evaluation of key genes which play a dominant role in the malignant development of ESCA.

Learning from our predecessors, we added the expression data from two microarrays to our research to enlarge the sample size, in order to reduce errors. We aimed to seek out hub genes and pathways involved in ESCA using integrated analysis of the chosen microarray data. Moreover, we aimed to conduct further expression and survival assessments of hub genes, which may provide reference and direction for early diagnosis and practical therapeutic strategies for ESCA. To our knowledge, the present study represents the first assessment of key hub genes associated with ESCA using bioinformatics methods to obtain information on altered expression of these genes at different stages, as well as their prognostic impact for diagnosed patients.

Material and Methods

Acquisition of datasets

The appropriate datasets were obtained from the Gene Expression Omnibus (GEO) database (<http://www.ncbi.nlm.nih.gov/geo>). Inclusion criteria were as follows: (1) sample from human esophageal tissue (cell-line and animal experiments excluded); (2) normalized expression data; (3) coverage of diverse types of ESCA, including ESCC, EAC, and rare types of ESCA; (4) control group from non-carcinoma oesophageal tissue; (5) inclusion of mRNA expression level.

After an overall scrutiny, the datasets of GSE100942 [15] and GSE111044 [16] were selected as they suited the inclusion standards we set up. Moreover, both of them had been created recently, in the past 5 years, which met the need for timeliness. GSE100942 consisted of ten samples, including five samples from ESCC and five samples from normal esophageal tissue. GSE111044 was made up of six samples, including three samples from small cell esophageal carcinoma (SCEC) and three samples from corresponding normal tissue.

Table 1. Details of DEGs filtered from GSE111044 and GSE100942.

Source	Total	Elements
Intersection of GSE111044 and GSE100942	210	SLMAP, SAMD4A, KCNMA1, LDB3, LINC01279, TPX2, EPB41L4B, WISP2, IGF2BP3, CCNB1, MSRB3, ANP32E, NFIA, CNN1, COL1A1, ANLN, BIRC5, GHR, BCHE, DNMT3B, SMAD9, LRRK2, HLF, ADAMTS2, AURKA, KIF14, FHL1, SORBS2, ADRB1, CSRP1, TCF21, KIF4A, KIT, RAD54B, C1QTNF7, NEGR1, FAM72A, KCNAB1, MELK, CDH11, NDC80, CCNA2, GTSE1, NUF2, KRT78, PDK4, MMP1, MYOCD, EPCAM, ANGPTL1, DAAM2, P2RY14, ECT2, KIF23, DEPDC1, EMCN, LPAR3, OGN, POSTN, NBEA, MYLK, CYSLTR1, CCNB2, PRC1, IGFBP6, TNXB, CEP55, MYOC, CCNE2, MCM2, MCM4, CGNL1, ADIRF, HEY1, SRPX, IL1RN, DLGAP5, RAD51AP1, SMTN, TMEM108, SCN7A, CCDC69, CDCA2, MYL9, LRRN4CL, RHPN2, CDH19, PGM5, SOBP, C2orf40, AOX1, COL1A2, LAPTM4B, GULP1, CFD, RNASE4, NEK2, ABLIM1, KIF26B, LPP, FGL2, CHRDL1, HSPB8, RAP1A, DEPDC1B, CILP, ITIH5, HMGB3, TMEM110, NETO2, SYNPO2, SOX4, PLN, MRVI1, EZH2, TNFSF10, CD36, CAPN14, CFH, MYOT, MT1M, RASEF, EMP1, PGM5-AS1, FAM149A, STEAP4, AOC3, LMOD1, ASPA, TMEM35A, CCL14, MYH11, KIF2C, EBF1, EREG, AGTR1, CDCA7, TNS1, CDC20, RBPM52, C7, BUB1, CCL2, PRR11, IL6, CPED1, RGS2, COL3A1, DPT, SCARA5, PTPRN2, ATP1A2, CDCA3, IFI6, ATAD2, KNL1, EXOSC7, ADAMTS1, ANOS1, SORBS1, FGF7, STIL, UBE2C, STXBP6, MTURN, CCDC80, CLU, CXCL12, IL36A, SLC35F6, TOP2A, AVPR1A, COL14A1, HELLS, FANCI, IRX2, NEXN, SPC25, KIF18A, BUB1B, DKK1, HJURP, AQP1, LMO3, SOCS2, DTL, ACTG2, ADH1B, MEST, ARHGAP6, HMMR, CAB39L, FAM107A, GPX3, KIF20A, SHISA2, ENC1, PTGS1, CASQ2, CTHRC1, UHRF1, SGO2, MAMDC2, TTK, CDKN3, NCAFG, FXD3, CENPF, NUSAP1, CRCT1



Figure 1. Venn diagram of filtered differentially expressed genes (DEGs) shared by the GSE111044 and GSE100942 datasets. The overlapping area, which contained 210 items, was considered to contain DEGs for ESCA.

Identification of DEGs

GEO2R (<http://www.ncbi.nlm.nih.gov/geo/geo2r/>), an online web tool affiliated with GEO, already provided access to the data set and collection. Further analysis was applied to the prepared datasets using GEO2R. The selected datasets were divided into two groups: the normal tissue group and the cancer group. Subsequently, direct statistical analysis of each dataset was conducted with cutoff values of: $p < 0.01$ and $2 |\log FC| \geq 3$. The intersection of the two filtered datasets, representing DEGs, was identified by a web-based tool named Venny v2.1. (<https://bioinfogp.cnb.csic.es/tools/venny/>).

Enrichment analysis

Gene ontology (GO) enrichment analysis was conducted using the online platform Metascape [17] (<http://metascape.org>). A set of functional classifications and annotations are included in Metascape, such as biological processes (BP), cellular components (CC), and molecular functions (MF). The norm for statistical significance of $p < 0.05$ was determined as the threshold value for our statistical analysis, to deeply screen enriched GO terms.

The Kyoto Encyclopedia of Genes and Genomes (KEGG) Orthology Based Annotation System, third version (KOBAS v3.0) [18] (<http://kobas.cbi.pku.edu.cn/kobas3>) was used to perform the KEGG pathway enrichment analysis. A corrected p value < 0.05 was considered to represent statistical significance. Moreover, we used the remaining pathways to draw a bubble chart of the top 20 pathways as a visualization, using OmicShare tools (<https://www.omicshare.com.html>).

Construction of the PPI network

The screened DEGs were imported into the Search Tool for the Retrieval of Interacting Genes (STRING) [19] (<http://string.embl.de/>) to begin network analysis. STRING possesses a potent ability to process multiple proteins or amino acid sequences input by users, which are then used to construct a protein-protein interaction (PPI) network. Conveniently, STRING can provide various types of exported files, including tsv, PNG, and tables. In our research, we downloaded the requisite files (tsv and PNG) to prepare for validation of hub genes and further research.

Table 2. GO enrichment analysis of ESCA-related DEGs.

Category	Term	Annotation	Count	P Value	FDR	
MF	GO: 0042393	Histone binding	5	0.040956	43.57063	
	GO: 0004672	Protein kinase activity	9	0.037858	41.02474	
	GO: 0017048	Rho GTPase binding	3	0.035287	38.83208	
	GO: 0008083	Growth factor activity	6	0.029217	33.3507	
	GO: 0003678	DNA helicase activity	3	0.026484	30.73641	
	GO: 0042826	Histone deacetylase binding	5	0.023265	27.53669	
	GO: 0019901	Protein kinase binding	10	0.019069	23.15887	
	GO: 0016887	ATPase activity	7	0.013453	16.91675	
	GO: 0048407	Platelet-derived growth factor binding	3	0.005775	7.618473	
	GO: 0005201	Extracellular matrix structural constituent	5	0.005574	7.362384	
	GO: 0005524	ATP binding	28	0.004315	5.745381	
	GO: 0008574	ATP-dependent microtubule motor activity, plus-end-directed	4	7.15E-04	0.97331	
	GO: 0008017	Microtubule binding	10	3.85E-04	0.525754	
	GO: 0008201	Heparin binding	9	3.10E-04	0.423032	
	GO: 0003777	Microtubule motor activity	7	2.05E-04	0.280292	
	GO: 0005515	Protein binding	118	1.98E-04	0.271172	
	GO: 0008307	Structural constituent of muscle	6	7.85E-05	0.107306	
	GO: 0003779	Actin binding	15	1.63E-06	0.002223	
	CC	GO: 0005814	Centriole	5	0.034311	36.49999
		GO: 0097149	Centralspindlin complex	2	0.032082	34.56688
GO: 0005694		Chromosome	5	0.0272	30.14128	
GO: 0070062		Extracellular exosome	42	0.0257	28.72761	
GO: 0005680		Anaphase-promoting complex	3	0.025342	28.38631	
GO: 0005584		Collagen type i trimer	2	0.021504	24.62943	
GO: 0016363		Nuclear matrix	5	0.021056	24.17972	
GO: 0051233		Spindle midzone	3	0.017618	20.64245	
GO: 0005925		Focal adhesion	11	0.010247	12.53825	
GO: 0015629		Actin cytoskeleton	8	0.009682	11.8868	
GO: 0005654		Nucleoplasm	44	0.008794	10.8543	
GO: 0005576		Extracellular region	29	0.008174	10.12583	
GO: 0048471		Perinuclear region of cytoplasm	15	0.007728	9.598831	
GO: 0005813		Centrosome	12	0.006822	8.519486	
GO: 0000922		Spindle pole	6	0.006621	8.277421	
GO: 0015630		Microtubule cytoskeleton	7	0.003771	4.795012	
GO: 0001725		Stress fiber	5	0.002747	3.514485	
GO: 0045120		Pronucleus	3	0.002356	3.021411	
GO: 0005737		Cytoplasm	77	0.001617	2.083603	
GO: 0005829		Cytosol	54	0.00154	1.984823	
GO: 0031012	Extracellular matrix	11	0.001477	1.904168		

Table 2 continued. GO enrichment analysis of ESCA-related DEGs.

Category	Term	Annotation	Count	P Value	FDR
CC [continued]	GO: 0005876	Spindle microtubule	5	0.001282	1.655013
	GO: 0031262	Ndc80 complex	3	6.88E-04	0.890813
	GO: 0000942	Condensed nuclear chromosome Outer kinetochore	3	6.88E-04	0.890813
	GO: 0005874	Microtubule	12	5.90E-04	0.765086
	GO: 0030018	Z disc	8	2.97E-04	0.385939
	GO: 0005581	Collagen trimer	8	6.25E-05	0.081295
	GO: 0000776	Kinetochore	8	2.74E-05	0.035668
	GO: 0005871	Kinesin complex	7	2.22E-05	0.028929
	GO: 0005615	Extracellular space	33	2.02E-05	0.026247
	GO: 0005578	Proteinaceous extracellular matrix	14	7.32E-06	0.009524
	GO: 0005819	Spindle	10	6.68E-06	0.008694
	GO: 0000775	Chromosome, centromeric region	8	2.59E-06	0.003375
	GO: 0030496	Midbody	11	1.40E-06	0.001819
	GO: 0000777	Condensed chromosome kinetochore	11	3.37E-08	4.38E-05
	BP	GO: 0007015	Actin filament organization	4	0.048188
GO: 0051436		Negative regulation of ubiquitin- protein ligase activity involved in mitotic cell cycle	4	0.046554	54.41983
GO: 0001666		Response to hypoxia	6	0.046026	54.00186
GO: 0046777		Protein autophosphorylation	6	0.046026	54.00186
GO: 0044344		Cellular response to fibroblast growth factor stimulus	3	0.045033	53.20648
GO: 2000660		Negative regulation of interleukin-1- mediated signaling pathway	2	0.044501	52.77484
GO: 0010574		Regulation of vascular endothelial growth factor production	2	0.044501	52.77484
GO: 0043154		Negative regulation of cysteine-type endopeptidase activity involved in apoptotic process	4	0.043372	51.8463
GO: 0097421		Liver regeneration	3	0.042339	50.98273
GO: 0051384		Response to glucocorticoid	4	0.037348	46.59797
GO: 0060326		Cell chemotaxis	4	0.037348	46.59797
GO: 0007049		Cell cycle	7	0.037147	46.41426
GO: 0045840		Positive regulation of mitotic nuclear division	3	0.034645	44.07219
GO: 0071173		Spindle assembly checkpoint	2	0.033564	43.03115
GO: 0060414		Aorta smooth muscle tissue morphogenesis	2	0.033564	43.03115
GO: 0006977		DNA damage response, signal transduction by p53 class mediator resulting in cell cycle arrest	4	0.033134	42.61195
GO: 0000070		Mitotic sister chromatid segregation	3	0.032215	41.70664
GO: 0006306		DNA methylation	3	0.032215	41.70664

Table 2 continued. GO enrichment analysis of ESCA-related DEGs.

Category	Term	Annotation	Count	P Value	FDR
BP [continued]	GO: 0042787	Protein ubiquitination involved in ubiquitin-dependent protein catabolic process	6	0.030104	39.57493
	GO: 0051966	Regulation of synaptic transmission, glutamatergic	3	0.02757	36.92013
	GO: 0051439	Regulation of ubiquitin-protein ligase activity involved in mitotic cell cycle	3	0.02757	36.92013
	GO: 0043547	Positive regulation of GTPase activity	13	0.027349	36.68291
	GO: 0070301	Cellular response to hydrogen peroxide	4	0.026698	35.9813
	GO: 1903779	Regulation of cardiac conduction	4	0.0255	34.66984
	GO: 0008283	Cell proliferation	10	0.023601	32.53933
	GO: 0048146	Positive regulation of fibroblast proliferation	4	0.023193	32.07322
	GO: 0000022	Mitotic spindle elongation	2	0.022502	31.27789
	GO: 0001501	Skeletal system development	6	0.019827	28.11186
	GO: 0010881	Regulation of cardiac muscle contraction by regulation of the release of sequestered calcium ions	3	0.019192	27.33961
	GO: 0006939	Smooth muscle contraction	3	0.017299	24.99359
	GO: 0051726	Cell cycle regulation	6	0.013422	19.96503
	GO: 0031145	Anaphase-promoting complex-dependent catabolic process	5	0.012345	18.5125
	GO: 0006957	Complement activation, alternative pathway	3	0.009152	14.06012
	GO: 0051310	Metaphase plate congression	3	0.007801	12.10953
	GO: 0055119	Relaxation of cardiac muscle	3	0.007801	12.10953
	GO: 0048565	Digestive tract development	4	0.007152	11.1566
	GO: 0008284	Positive regulation of cell proliferation	13	0.006888	10.76681
	GO: 0030574	Collagen catabolic process	5	0.005947	9.363414
	GO: 0034501	Protein localization to kinetochore	3	0.005399	8.535467
	GO: 0032060	Bleb assembly	3	0.005399	8.535467
	GO: 0007019	Microtubule depolymerization	3	0.005399	8.535467
	GO: 0006268	DNA unwinding involved in DNA replication	3	0.005399	8.535467
	GO: 0009612	Response to mechanical stimulus	5	0.00445	7.087078
	GO: 0071549	Cellular response to dexamethasone stimulus	4	0.004196	6.694943
	GO: 0019221	Cytokine-mediated signaling pathway	7	0.003769	6.034147
	GO: 0032355	Response to estradiol	6	0.00373	5.973802
	GO: 0001558	Regulation of cell growth	6	0.00213	3.453634
	GO: 0000910	Cytokinesis	5	0.002095	3.397158
	GO: 0007094	Mitotic spindle assembly checkpoint	4	0.00141	2.299434

Table 2 continued. GO enrichment analysis of ESCA-related DEGs.

Category	Term	Annotation	Count	P Value	FDR
BP [continued]	GO: 0000086	G2/M transition of mitotic cell cycle	8	9.49E-04	1.552707
	GO: 0007080	Mitotic metaphase plate congression	5	7.83E-04	1.283031
	GO: 0007155	Cell adhesion	15	7.52E-04	1.232171
	GO: 0007018	Microtubule-based movement	7	3.11E-04	0.511889
	GO: 0030199	Collagen fibril organization	6	7.41E-05	0.122099
	GO: 0006936	Muscle contraction	9	2.91E-05	0.047888
	GO: 0007052	Mitotic spindle organization	6	1.99E-05	0.032833
	GO: 0000281	Mitotic cytokinesis	6	1.68E-05	0.027614
	GO: 0007059	Chromosome segregation	8	1.15E-05	0.018962
	GO: 0007062	Sister chromatid cohesion	12	2.35E-08	3.87E-05
	GO: 0007067	Mitotic nuclear division	20	5.66E-11	9.33E-08
	GO: 0051301	Cell division	25	1.55E-12	2.55E-09

Expression analysis of hub genes

In light of degree level, hub genes were identified by cytohubba, an analytic tool attached to Cytoscape software [20] (<https://cytoscape.org/>). Cytohubba can rank nodes in a network by their network features in order to find a requested objective from imported elements of a PPI network, at levels of degree, closeness, and so on.

We successfully used Gene Expression Profiling Interactive Analysis (GEPIA2) [21] (<http://gepia2.cancer-pku.cn>) to compare mRNA expression levels between ESCA tissue and paired normal tissue. Additionally, differential expression levels in patients at each stage of ESCA were compared in GEPIA.

Survival analysis of hub genes

Oncolnc [22] (<http://www.oncolnc.org/>) was used to analyze predictive hub gene data. Oncolnc is an efficient online analytic box, which can supply survival data correlated with mRNA expression level based on The Cancer Genome Atlas (TCGA) data. We set 50 as the cutoff to divide paired data into high- and low-expression groups, for a Kaplan plot of input genes related to ESCA.

Results

Confirmation of DEGs

After GEO2R analysis of the two screened datasets, the criterion $p < 0.01$ and $2 |\log FC| \geq 3$ was utilized for statistical analysis. A total of 3170 and 318 gene fragments were selected from the GSE111044 and GSE100942 datasets. Genes found to be

present in both datasets were selected as DEGs. Consequently, a total of 210 DEGs were screened from the two genetic datasets (Table 1, Figure 1).

GO enrichment analysis

In total, 114 GO terms mediated by the DEGs were identified as enriched, spanning the categories of molecular function (MF), cellular component (CC), and biological process (BP) (Table 2). The MF results implicated DEGs that were profoundly enriched in actin binding, extracellular matrix structural constituents, and structural constituents of muscle (Figure 2). The CC results indicated that DEGs were enriched in chromosome, centromere, spindle, extracellular matrix, and stress fibers (Figure 3). With respect to BP, DEGs were noticeably enriched in processes related to cell division, mitotic cell cycle phase transition, muscle system process, and muscle structural development (Figure 4). We then obtained the top 20 terms of the GO functional enrichment analysis (Figure 5). The results indicated that ESCA-related DEGs were mainly involved in cell division, muscle system process, development and attachment of spindle microtubules to the kinetochore at the midbody, and extracellular matrix.

Enrichment analysis of the KEGG pathway

In total, 107 pathways connected with DEGs were procured through KOBAS v3.0. The corrected p value < 0.05 was set as the statistical cutoff, and 60 pathways without statistical difference were rejected. The remaining 47 pathways with statistical significance are presented in Table 3. Among these remaining pathways, we chose the top 20 enriched pathways using OmicShare tools (Figure 6). These pathways revealed that a broad spectrum of DEGs participated in the cell cycle,

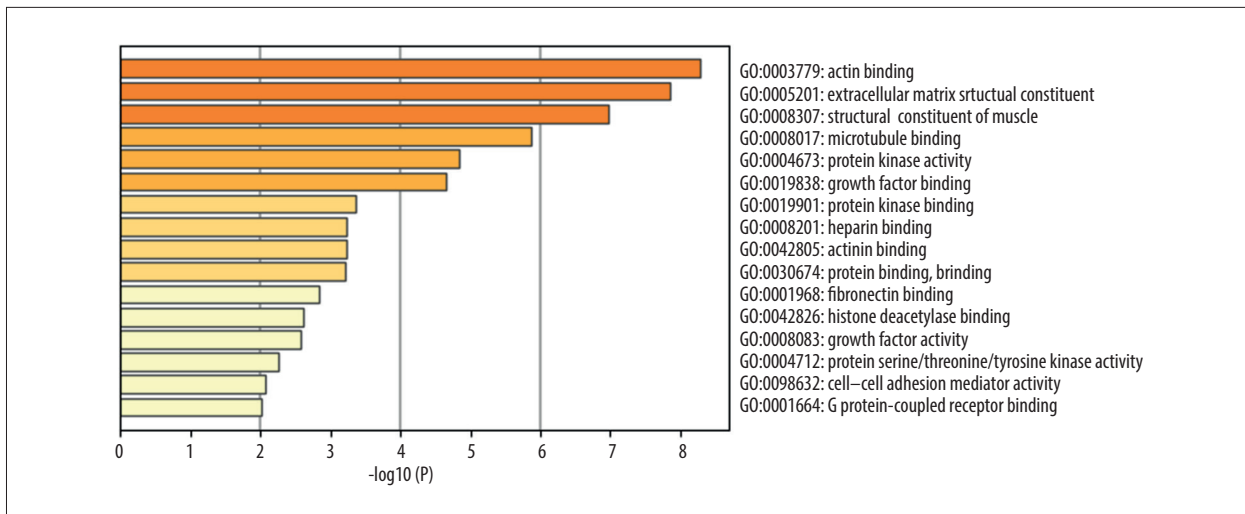


Figure 2. Top 16 enriched molecular function GO terms. The horizontal axis is a logarithmic calculation of p value, while GO terms are listed on the y axis. The length of each bar represents lower p value (higher significance). Actin binding was the term with the highest significance level.

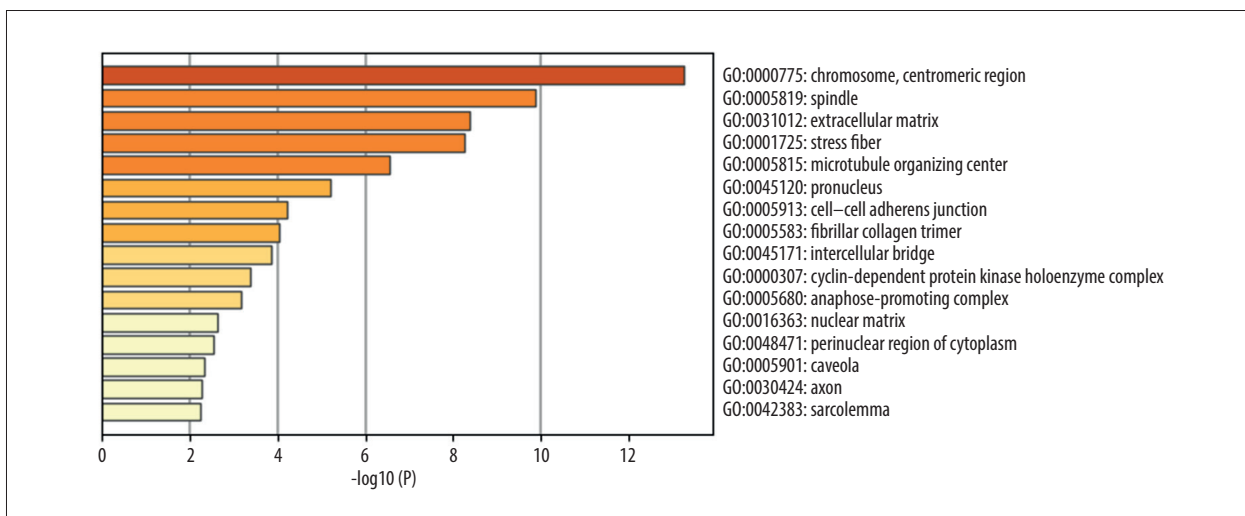


Figure 3. Top 16 enriched cellular component GO terms. The horizontal axis is a logarithmic calculation of p value, while GO terms are listed on the y axis. The length of each bar represents lower p value (higher significance). Chromosome and centromeric region was the term with the highest significance level.

pathways in cancer, the phosphatidylinositol-3-kinase (PI3K)/protein kinase B (AKT) signaling pathway, the cGMP-protein kinase G (PKG) signaling pathway, cytokine-cytokine receptor interaction, and vascular smooth muscle contraction.

Construction of the PPI network and identification of hub genes

The PPI network exported by STRING comprised 202 nodes and 1571 edges (Figure 7). The modular interaction network was viewed as statistically enriched, due to the enrichment p value <1.0e-16 (<0.05). The top 10 genes in the PPI network, in terms of degree ranking, were regarded as hub genes (Figure 8);

these genes probably play crucial roles in the incidence and development of ESCA. TOP2A was in the highest rank among all the DEGs, followed by UBE2C, BUB1, KIF20A, TTK, CCNB2, KIF2C, TPX2, CCNA2, and CCNB1.

Expression analysis of hub genes

The expression boxplots of the hub genes, conveyed on the basis of TCGA and GTEx data, demonstrated that these hub genes were upregulated in ESCA tissue compared with normal esophageal tissue (Figure 9). Further, we evaluated the expression level of the hub genes at different pathological stages among ESCA patients (stage I, stage II, stage III, and stage IV

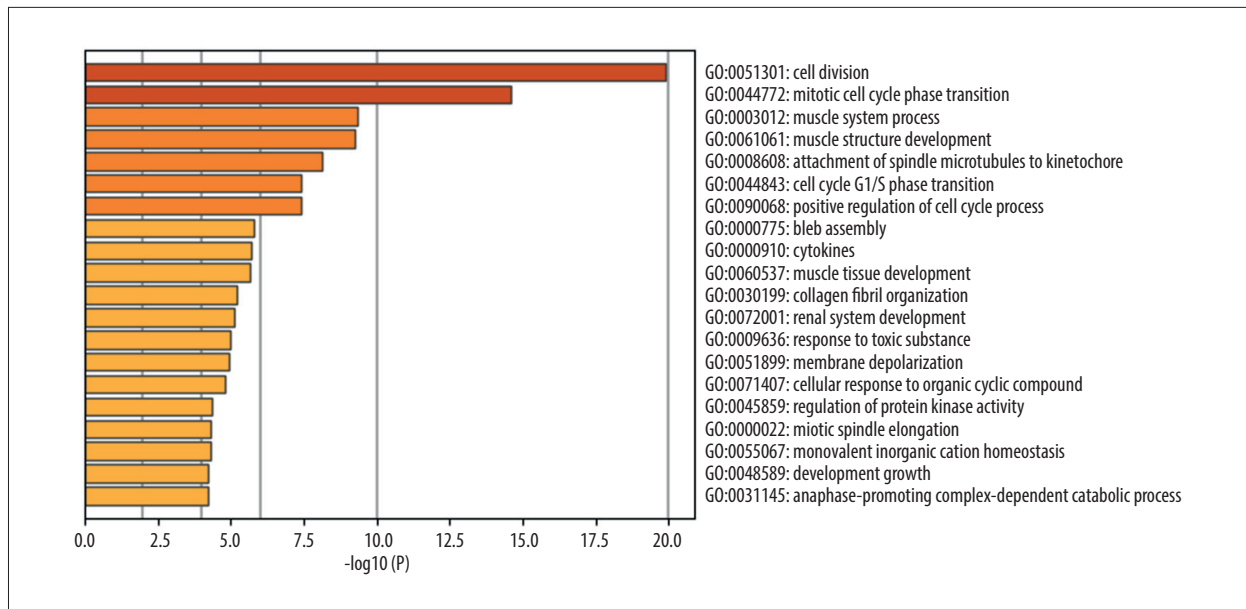


Figure 4. Top 20 enriched biological process GO terms. The horizontal axis is a logarithmic calculation of p value, while GO terms are listed on the y axis. The length of each bar represents lower p value (higher significance). Cell division was the term with the highest significance level.

patients). The stage-plots were scored using GEPIA (Figure 10). As is shown below, the expression level of the hub genes differed at different stages.

Survival analysis for the hub genes

The survival curve output by OncoLnc showed that all the hub genes with high expression, in comparison with those with low expression, improved the percentage of late survival, after the 2000-day timepoint (>2000 on the x axis) (Figure 11). Moreover, when the surviving percentile of ESCA patients was stationary, high expression of the hub genes prolonged survival time. However, the hub genes exhibited few associations with early survival.

Discussion

ESCA is a major global health challenge with multifactorial etiology, including both genetic and environmental components. Efforts to detect inchoate changes have attenuated the development of malignant cancer, and have even had some success in prevention [9]. Therefore, it is of vital importance to seek out predictive indicators and therapeutic markers for ESCA.

In our research, 210 DEGs were screened from two genetic expression datasets, via the GEO bioinformatics portal. Then, GO function enrichment analysis and KEGG pathway enrichment analysis were applied to filter the DEGs. A PPI network was constructed using STRING to obtain hub genes that are likely

to be central to the ESCA pathological process. Most previous studies in this field stopped at this point, resulting in limited clinical usefulness. Therefore, we implemented further analysis targeting the crucial hub genes identified in the first steps of our study. We focused on the assessment of screened hub genes with greater possibility as new therapeutic targets for treating ESCA. We conducted expression analysis of these hub genes in patients at different stages of ESCA, as well as prognostic analysis. These analyses showed the potential of these hub genes as biomarkers for appraisal in the process of therapy and post-therapy.

The results of GO functional enrichment analysis identified several DEGs exhibiting a distinction from genes expressed in healthy esophageal tissue. The DEGs were principally targeted to the midbody, with functions related to cell division and attachment of spindle microtubules to the kinetochore. The results suggested that multitudes of DEGs were closely associated with nuclear activities, especially cell division. Cell division as a functional category includes mechanisms to properly orient and position the mitotic spindle, which is important because incorrect activity related to the spindle contributes to disease, even carcinogenesis [23,24]. Echoing the KEGG pathway enrichment analysis, the DEGs were strongly related to the cell cycle. Dysregulation of the cell cycle leading to endless proliferation of cells has been implicated in tumorigenesis [25]. Jing Wen et al. [26] found that, *in vitro* and *in vivo*, transcriptional activation of miR-424 elevated proliferation of ESCC cell lines and led to poor survival in ESCC patients; this activation facilitates both G1/S and G2/M cell cycle

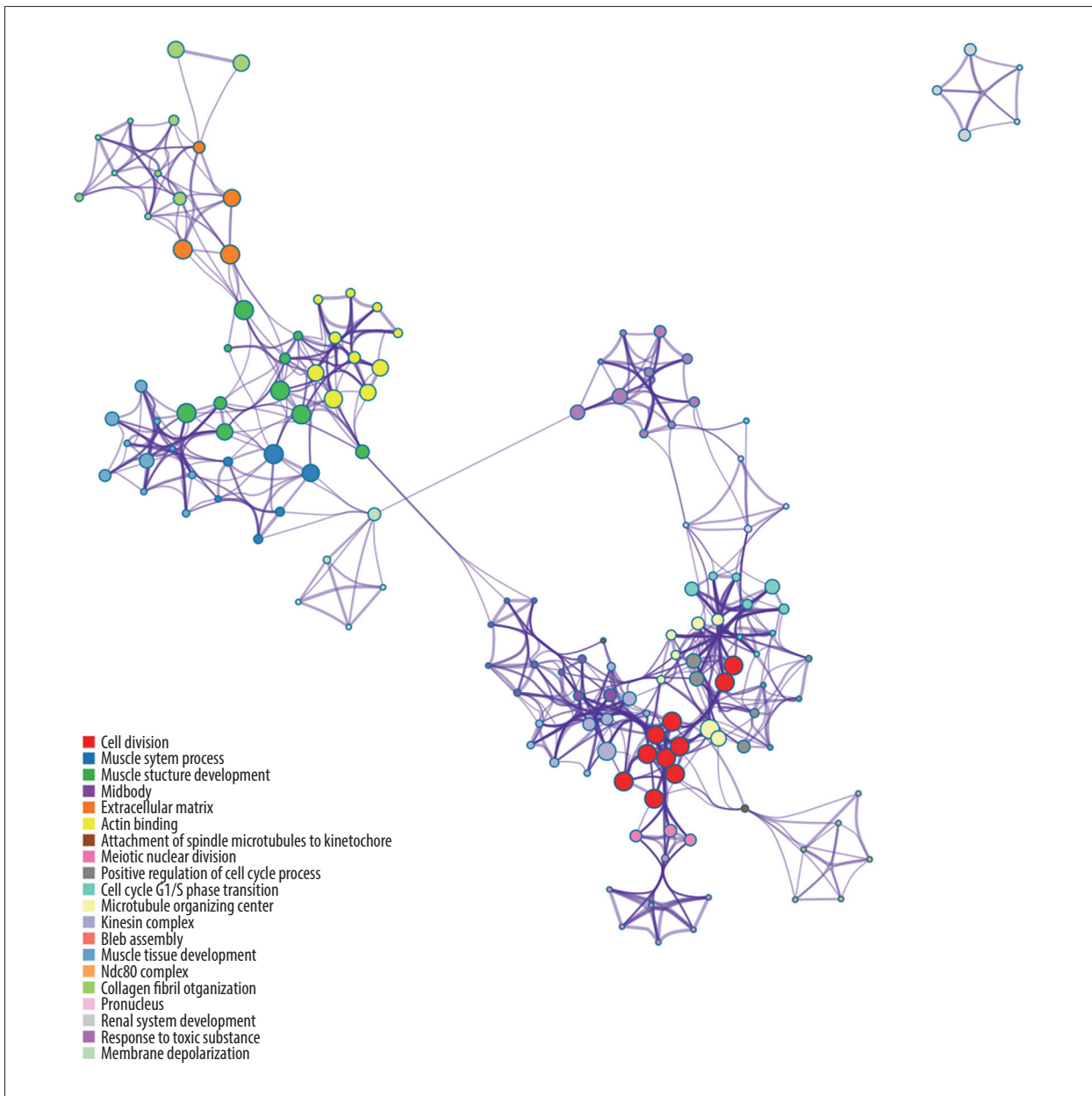


Figure 5. Top 20 results from GO functional enrichment analysis. The size of the filled circles indicates statistical significance. Larger circle size indicates lower p value. Circle color indicates type of GO term, as listed in the legend (lower left corner).

transitions. However, inhibition of cell cycle progression alleviates the development of malignancy. Chinese researchers have demonstrated that a novel Notch inhibitor called FLI-06 exerts antitumor activity in a dose-dependent manner via cell-cycle arrest and proliferation suppression in ESCC cells [27]. Above all, therapeutic interventions targeting cell division may generate antitumor activity.

Additionally, the KEGG pathway enrichment analysis showed that the DEGs were enriched in the PI3K-Akt signaling pathway, the cGMP-PKG signaling pathway, cytokine-cytokine

receptor interaction, and vascular smooth muscle contraction. Intriguingly, those findings differed from those of a similar study using bioinformatics methods conducted by He et al. [25]. Their findings indicated that DEGs related to ECA were mainly enriched in complement and coagulation cascades, mature-onset diabetes in the young, and retinol metabolism. Given that their sample was extracted from ECA patients and ours from patients diagnosed with ESCC and SCEC, it was inevitable for the two studies to find differences. Still, the evidence supporting our scientific results are as follows:

Table 3. KEGG pathway enrichment analysis of ESCA-related DEGs.

Term	Number	Corrected p value	Genes
Cell cycle	10	1.19E-08	CCNB2, CCNB1, CCNA2, BUB1B, CCNE2, CDC20, TTK, MCM4, MCM2, BUB1
cGMP-PKG signaling pathway	9	1.51E-06	MRVI1, MYLK, KCNMA1, ADRB1, ATP1A2, RGS2, PLN, AGTR1, MYL9
Vascular smooth muscle contraction	8	2.68E-06	MYH11, MRVI1, AVPR1A, ACTG2, MYLK, KCNMA1, AGTR1, MYL9
AGE-RAGE signaling pathway in diabetic complications	6	0.000105714	CCL2, IL6, COL1A2, COL1A1, COL3A1, AGTR1
Pathways in cancer	11	0.00016471	CXCL12, CCNE2, BIRC5, KIT, IL6, HLF, FGF7, LPAR3, AGTR1, HEY1, MMP1
PI3K-Akt signaling pathway	9	0.000181898	GHR, CCNE2, KIT, IL6, COL1A2, EREG, COL1A1, FGF7, LPAR3
Platelet activation	6	0.000181898	PTGS1, MYLK, RAP1A, COL1A2, COL1A1, COL3A1
Calcium signaling pathway	7	0.000181898	AVPR1A, CASQ2, MYLK, ADRB1, PLN, AGTR1, CYSLTR1
Oocyte meiosis	6	0.000181898	CCNB2, CCNB1, BUB1, CCNE2, CDC20, AURKA
Cytokine-cytokine receptor interaction	8	0.000256568	CCL2, IL1RN, TNFSF10, GHR, DTL, IL6, IL36A, CXCL12
Protein digestion and absorption	5	0.000372719	COL3A1, COL14A1, COL1A2, ATP1A2, COL1A1
Rheumatoid arthritis	5	0.000372719	IL6, CCL2, CXCL12, DTL, MMP1
Progesterone-mediated oocyte maturation	5	0.000505745	CCNB2, CCNB1, CCNA2, AURKA, BUB1
p53 signaling pathway	4	0.001955985	CCNE2, CCNB2, CCNB1, GTSE1
Human T-cell leukemia virus 1 infection	6	0.001955985	CCNB2, CCNA2, BUB1B, CCNE2, CDC20, IL6
Adrenergic signaling in cardiomyocytes	5	0.002613273	ADRB1, AGTR1, SCN7A, ATP1A2, PLN
Neuroactive ligand-receptor interaction	7	0.002678945	AVPR1A, GHR, P2RY14, ADRB1, LPAR3, AGTR1, CYSLTR1
ECM-receptor interaction	4	0.003021888	HMMR, COL1A2, CD36, COL1A1
Cellular senescence	5	0.003023275	IL6, CCNB2, CCNB1, CCNE2, CCNA2
Jak-STAT signaling pathway	5	0.003030745	IL6, AOX1, FHL1, GHR, SOCS2
Tyrosine metabolism	3	0.003030745	AOX1, AOC3, ADH1B
Amoebiasis	4	0.003552075	IL6, COL3A1, COL1A2, COL1A1
Viral protein interaction with cytokine and cytokine receptor	4	0.004092655	IL6, CCL2, CXCL12, TNFSF10
Malaria	3	0.005771037	IL6, CCL2, CD36
Intestinal immune network for IgA production	3	0.005771037	IL6, CXCL12, DTL
Focal adhesion	5	0.005771037	MYL9, COL1A2, MYLK, RAP1A, COL1A1
cAMP signaling pathway	5	0.007342941	ADRB1, MYL9, ATP1A2, RAP1A, PLN
Regulation of actin cytoskeleton	5	0.007342941	FGF7, CFD, CXCL12, MYLK, MYL9
Relaxin signaling pathway	4	0.008337936	COL3A1, COL1A1, COL1A2, MMP1

Table 3 continued. KEGG pathway enrichment analysis of ESCA-related DEGs.

Term	Number	Corrected p value	Genes
FoxO signaling pathway	4	0.008510363	IL6, CCNB2, CCNB1, TNFSF10
Renin secretion	3	0.011964411	ADRB1, AGTR1, KCNMA1
Phospholipase D signaling pathway	4	0.011964411	LPAR3, AGTR1, AVPR1A, KIT
PPAR signaling pathway	3	0.015020846	SORBS1, CD36, MMP1
Hepatitis B	4	0.015736213	IL6, CCNE2, BIRC5, CCNA2
Complement and coagulation cascades	3	0.015736213	CLU, C7, CFH
Tight junction	4	0.017269759	MYH11, EPB41L4B, RAP1A, MYL9
Salivary secretion	3	0.021192296	ADRB1, KCNMA1, ATP1A2
MicroRNAs in cancer	5	0.021964309	DNMT3B, CCNE2, EZH2, KIF23, SOX4
IL-17 signaling pathway	3	0.021964309	IL6, CCL2, MMP1
Hematopoietic cell lineage	3	0.023983878	IL6, CD36, KIT
Pancreatic secretion	3	0.024052267	KCNMA1, RAP1A, ATP1A2
Human papillomavirus infection	5	0.029816413	CCNE2, CCNA2, COL1A1, COL1A2, HEY1
Rap1 signaling pathway	4	0.029816413	FGF7, LPAR3, RAP1A, KIT
Prion diseases	2	0.030030738	IL6, C7
DNA replication	2	0.03062247	MCM4, MCM2
Leukocyte transendothelial migration	3	0.03062247	CXCL12, RAP1A, MYL9
AMPK signaling pathway	3	0.035976653	CAB39L, CCNA2, CD36

The PI3K-Akt signaling pathway is implicated in several cancers, including breast cancer, colorectal carcinoma, hepatocellular cancer, and others [28–30]. Invariably, this pathway plays an important role in metastasis and prognosis among ESCA patients [31,32]. Ni Shi et al. [33] showed that MK2206/BEZ235 enhances apoptosis and inhibits tumor growth targeted at AKT phosphorylation in a mouse xenograft model of ESCC and *in vitro*. Moreover, the combination of MK2206 and BEZ235 boost antitumor effects because of dual PI3K and AKT inhibition. Another study demonstrated that Osthole, extracted from the herb *Cnidium monnieri* (L.) Cuss, reduced expression of PI3K and phosphorylated AKT (p-AKT), and thereby decreased ESCC proliferation [34]. Hence, treatments targeting the PI3K-Akt signaling pathway provide a promising approach to prevent ESCA and/or to slow its progression. The cGMP-PKG signaling pathway modulates massive physiological and pathological parameters [35]. Correlation between inflammation and the cGMP-PKG signaling pathway has been identified, involving mechanisms of neutrophil migration, mitochondrial permeability transition, and oscillations of calcium ions [36,37]. Interestingly, the mechanism responsible for dysplasia-induced (especially by Barrett’s esophagus) early EAC included a substantial promotion in the levels of inflammatory cytokines [38].

This implies that the cGMP-PKG signaling pathway is possibly connected with ESCA pathology in the early stages. Although studies testing the potential role of pharmacological modulation of the cGMP-PKG signaling pathway as an anticancer therapy are scant, we still hold a positive belief in their potential.

Tumor events are elicited by the collective expression of multiple genes, while single genes function as carcinogens particularly associated with severity [39]. As revealed in the PPI network, coordinated DEGs mediated the occurrence and development of ESCA. To select the critical genes for the interlaced construction, we input information for all DEGs to Cytoscape to screen the top 10 nodes in terms of degree. As a consequence, the degree of TOP2A ranked the highest, followed by UBE2C, BUB1, KIF20A, TTK, CCNB2, KIF2C, TPX2, CCNA2, and CCNB1. These nodes were regarded as hub genes for ESCA. In contrast, He et al. [25] identified IL8, IVL, TIMP1, FN1, SERPINE1, SERPINA1, CFTR, SPP1, COL1A1, and AGT as hub genes for ESCA. They focused on EAC while we focused on ESCC and SCEC. It has been established that there are substantial differences between EAC and ESCC, especially in terms of pathology [3], so it is not surprising to obtain distinct results. Taken together, all 10 hub genes we identified were linked to cell proliferation,

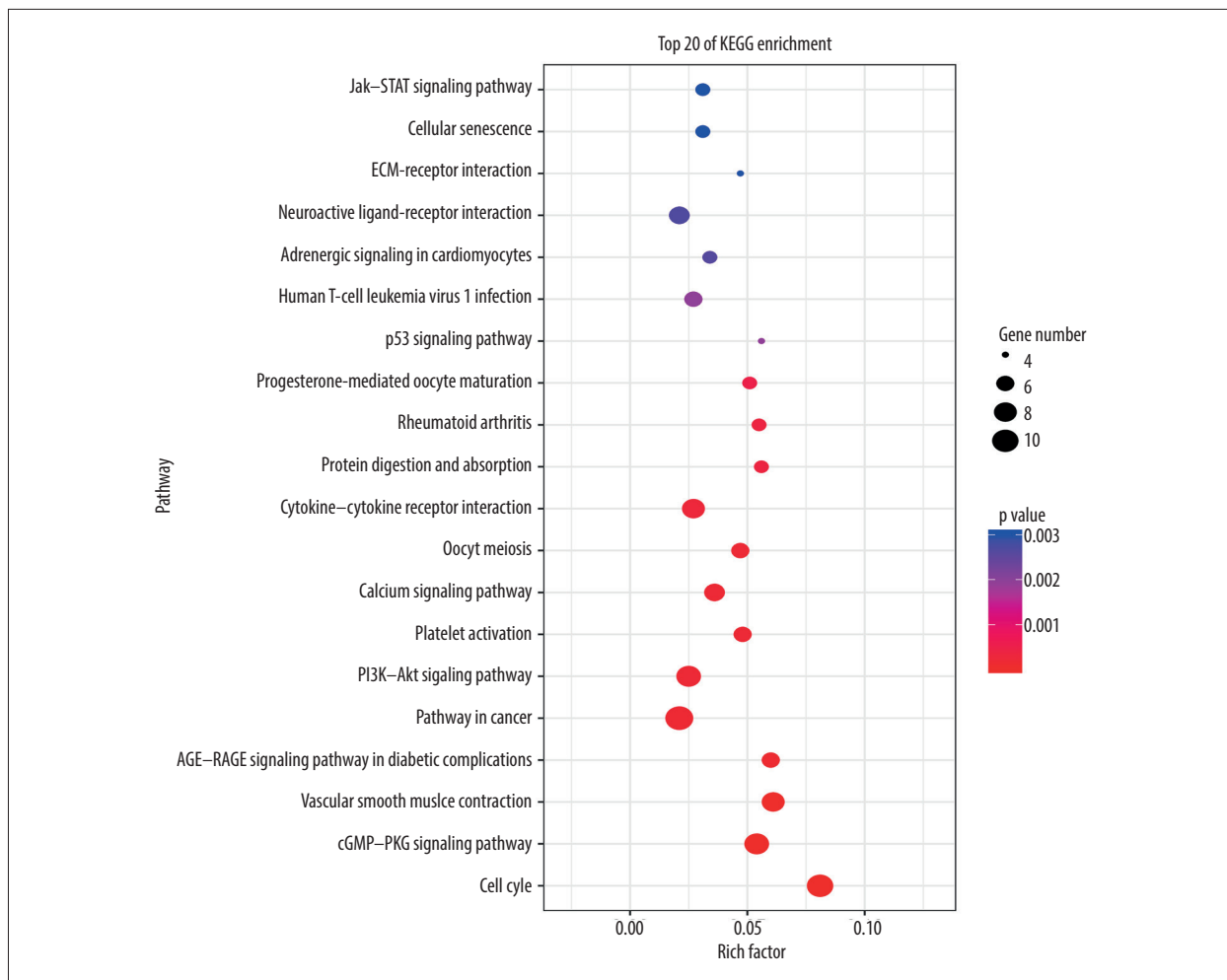


Figure 6. The top 20 KEGG pathways involving the differentially expressed genes (DEGs). Rich factor is represented on the x axis. KEGG pathway annotation is represented on the y axis. The size of the filled circles symbolizes the number of genes involved in the pathways. The color of the filled circles denotes significance, with gradation from red to blue symbolizing increasing p value.

involving the cell cycle or chromosome activity. Details about key hub genes are demonstrated as follows:

CCNA2 controls both the G1/S and the G2/M transition phases of the cell cycle, via the formation of specific serine/threonine protein kinase holoenzyme complexes with the cyclin-dependent protein kinases CDK1 or CDK2 [40]. Emerging evidence indicates that miR-219-5p mitigates ESCC cell proliferation by decreasing expression levels of CCNA2. Knockdown of CCNA2 enhances the impacts of miR-219-5p in terms of cell proliferation and cell cycle process [41]. CCNB2 and CCNB1 are elementary parts of the G2/M (mitosis) transition. One of the reasons why the overexpression of erythrocyte membrane protein band 4.1 like 3 (EPB41L3) noticeably improved overall survival rates among ESCA patients was its activation of CCNB1 signaling to induce G2/M cell cycle arrest [42]. A number of studies have found the high expression of CCNB2 to be

related to tumor growth and poor prognosis in several cancers, including non-small cell lung carcinomas (NSCLC), hepatocellular carcinoma, and gastric cancer [43–45]. Without laboratory data on ESCA, the role of CCNB2 is still controversial. Given that CCNB2, CCNA2, and CCNB1 are essential for cell cycle regulation, and are subsidiary to the cyclin family, they have potential as therapeutic targets for ESCA.

KIF20A and KIF2C are implicated in chromosome activity. They belong to the kinesin superfamily, and probably possess the potential to ameliorate malignancy. The kinesin family plays a significant role in microtubule motor activity of several cellular and extracellular structures, including Golgi membranes, chromosomes, associated vesicles along microtubules, and the central spindle [46]. KIF20A is a member of the kinesin-6 subfamily, and is crucial for cytokinesis and spindle assembly. Its expression pattern is linked to tumor development and

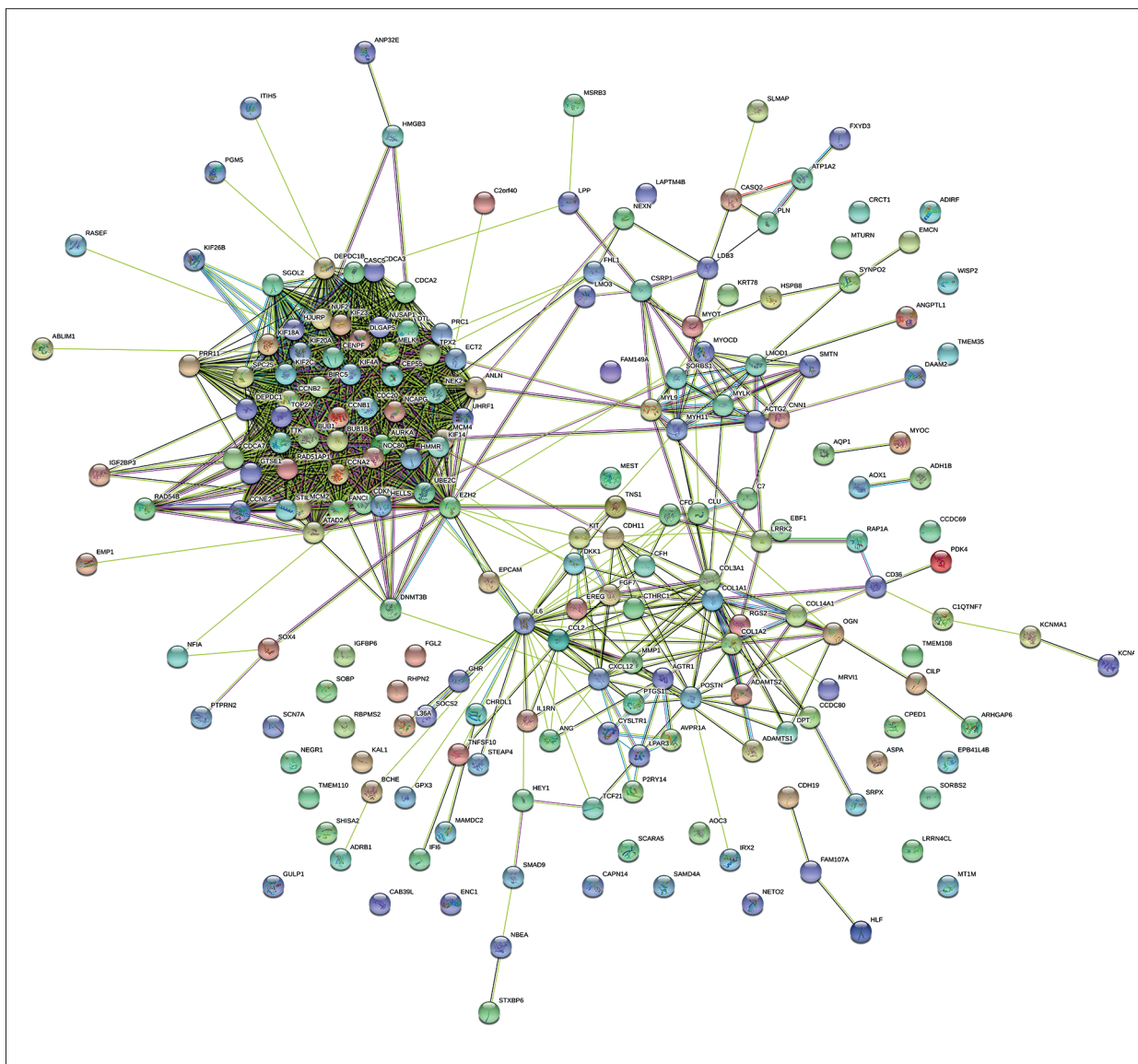


Figure 7. PPI network of ESCA-related differentially expressed genes (DEGs). The number of nodes was 202 (with 8 untouched genes). The number of edges was 1571; much higher than the expected 298 edges. The average node degree was 15.6. The average local clustering coefficient was 0.582. The PPI enrichment p value was less than $1.0e-16$.

prognosis [47]. KIF2C is responsible for the majority of microtubule plus-end depolymerizing activity in mitotic cells. It is required for chromosome segregation and congression during mitosis, and regulates the turnover and conversion of microtubules [48]. An immunohistochemical analysis conducted in ESCA tissue and adjacent non-cancerous tissues revealed that higher KIF2C expression led to higher pathologic tumor status and poorer tumor differentiation, but only for male patients [49].

TOP2A controls topological states of DNA, a crucial role for proper segregation of daughter chromosomes during mitosis and meiosis [50]. One clinical study suggested that high TOP2A could serve as a biomarker driving medical therapy [51]. Another

study showed that the knockdown of the long noncoding RNA (lncRNA) DDX11-AS1 reversed paclitaxel (PTX) resistance by means of inhibiting the expression level of TOP2A [52]. Both of these results imply that targeting the expression of TOP2A may have promise as a pharmacological treatment.

BUB1 is identified as a mitotic checkpoint that is important for spindle-assembly checkpoint signaling and correct chromosome alignment [53]. The transcriptional level of BUB1 in Barrett's patients, leading to early chromosomal instability (CI), can be helpful in EAC [54]. For the time being, we can hypothesize that treatment modifying BUB1 expression may benefit ESCA patients.

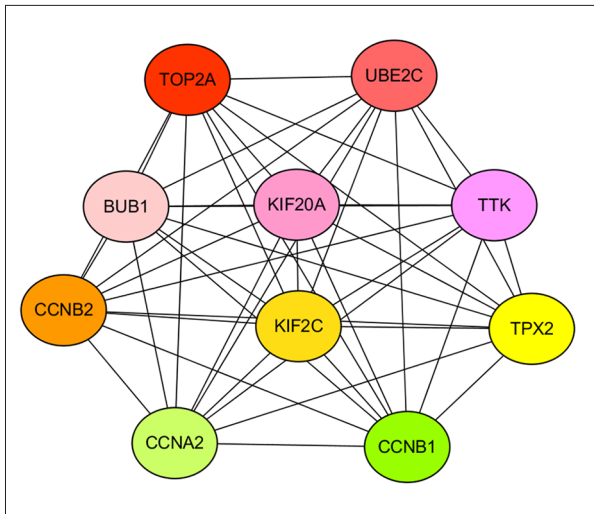


Figure 8. Topological diagram of the top 10 hub genes. In accordance with degree ranking, the top 10 differentially expressed genes (DEGs) were accepted as hub genes. Among all the DEGs, TOP2A was in the highest degree rank, followed by UBE2C, BUB1, KIF20A, TTK, CCNB2, KIF2C, TPX2, CCNA2, and CCNB1.

Meanwhile, the expression of UBE2C, TTK, and TPX2 is involved in ESCA pathology and prognosis. As a ubiquitin-conjugating enzyme, UBE2C promotes the degradation of several cell cycle-regulated proteins that control progression through mitosis [55]. Knockdown of UBE2C significantly inhibits cell proliferation via cell-cycle regulation, in *in-vitro* ESCA cell models, particularly in TE-1 cell lines [56]. TTK is associated with cell proliferation and chromosome alignment [57]. Previous clinical trials found that immunotherapies using epitope peptides derived from TTK potentiated cell response and immunity against ESCA [58,59]. TPX2 is required for normal assembly of microtubules as well as mitotic spindles during apoptosis. As detected by RT-qPCR, the relative expression of TPX2 is up-regulated in ESCA tumor tissue, and in lymph node metastasis [60]. Moreover, low expression of miR-491 aimed at TPX2 promotes cell invasion in ESCA clinical samples, affecting carcinogenesis and cancer development [61].

Collectively, we identified 210 DEGs and implemented GO analysis, KEGG pathway enrichment analysis, and PPI network construction to understand their possible roles in ESCA

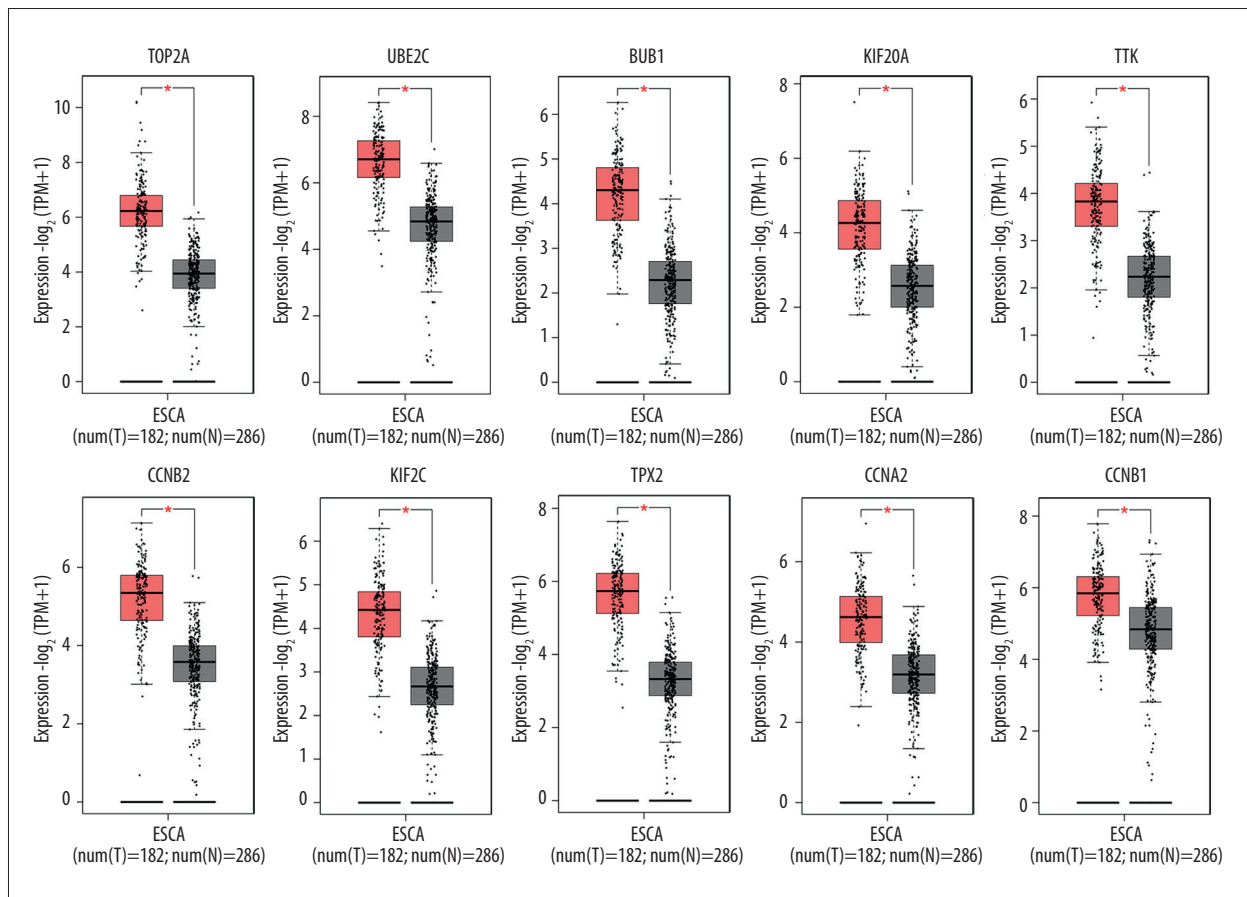
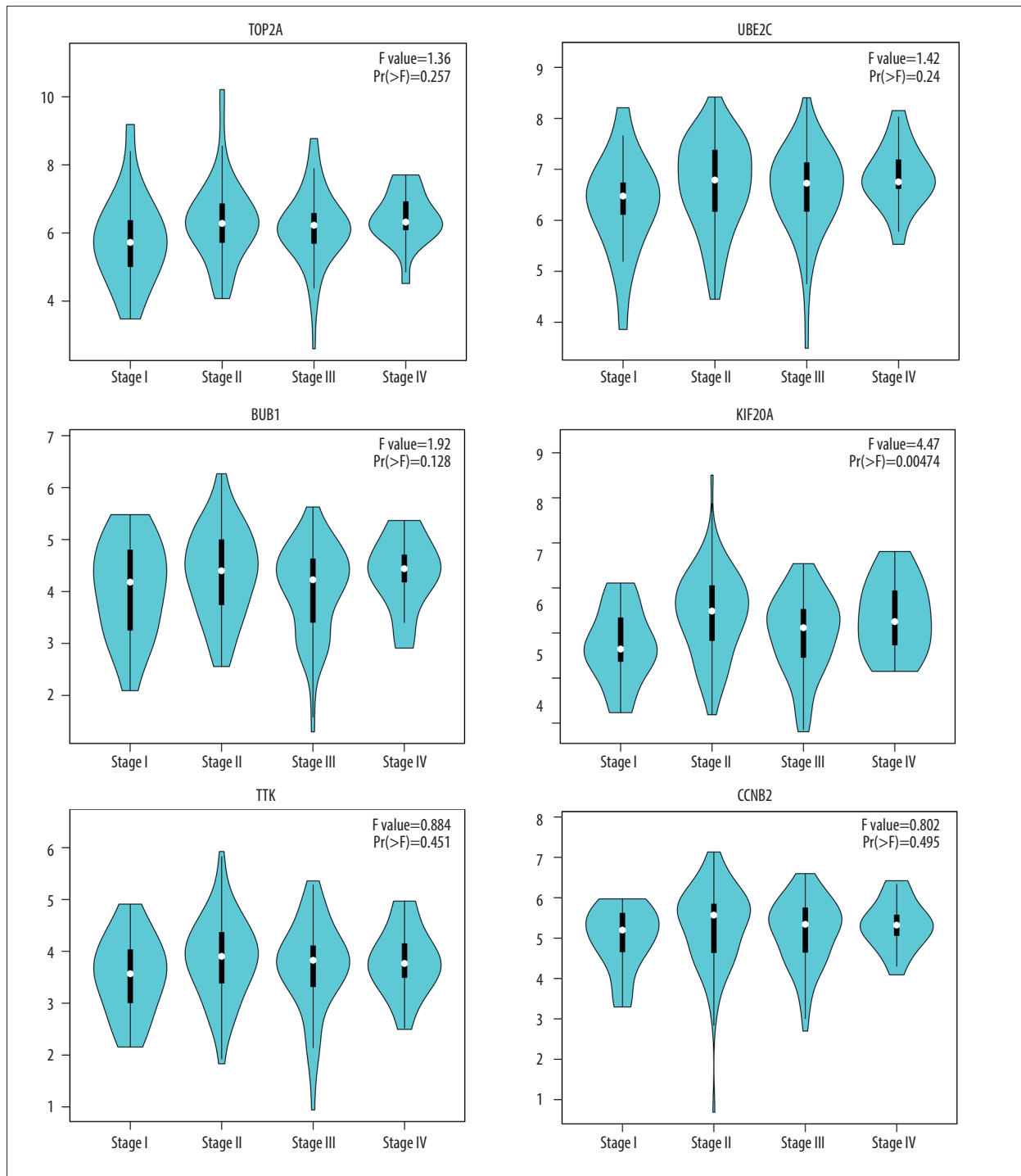


Figure 9. Differences in expression level of the top 10 hub genes between ESCA tissue and matched normal tissue. The plots are based on TCGA and GTEx data, and reveal that these hub genes are significantly upregulated in ESCA tissue compared with normal tissue ($p < 0.01$). The red * denotes statistically significant difference.

carcinogenesis. The enriched KEGG pathway implicated pathological mechanisms in ESCA, including the cell cycle and the PI3K-Akt and cGMP-PKG signaling pathways. Furthermore, we identified 10 hub genes and assessed their prognostic value. The 10 hub genes were TOP2A (highest ranking in terms of degree), UBE2C, BUB1, KIF20A, TTK, CCNB2, KIF2C, TPX2, CCNA2,

and CCNB1. These genes showed marked connections with late survival of ESCA patients, indicating their value in diagnosis and survival improvement.

Our research provides new insights for ESCA early diagnosis and survival evaluation, at the level of genes, pathways, and



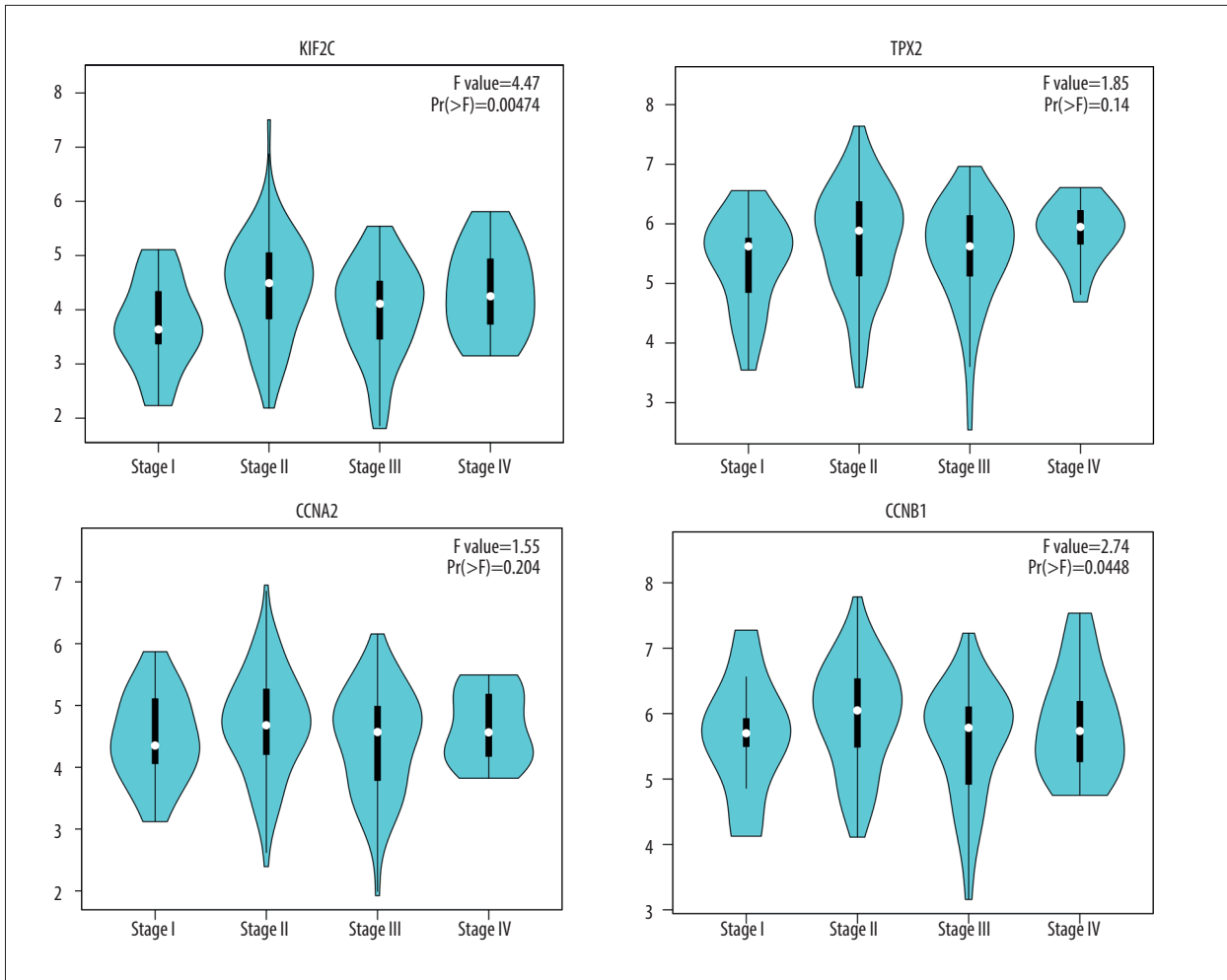
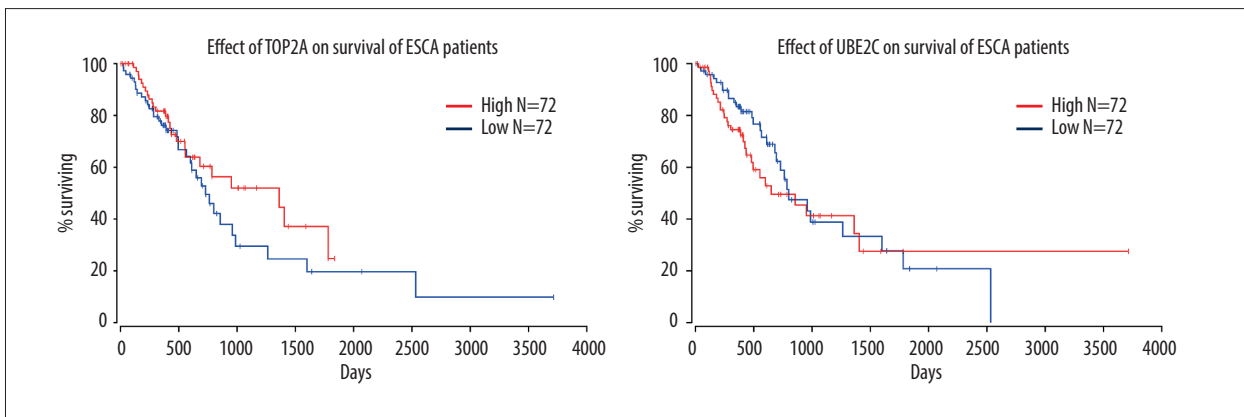


Figure 10. GEPIA stage-plots for the top 10 hub genes in patients at different stages of ESCA. The stage-plot is considered statistically significant when $Pr > F$. Greater F values represent increasing significance.



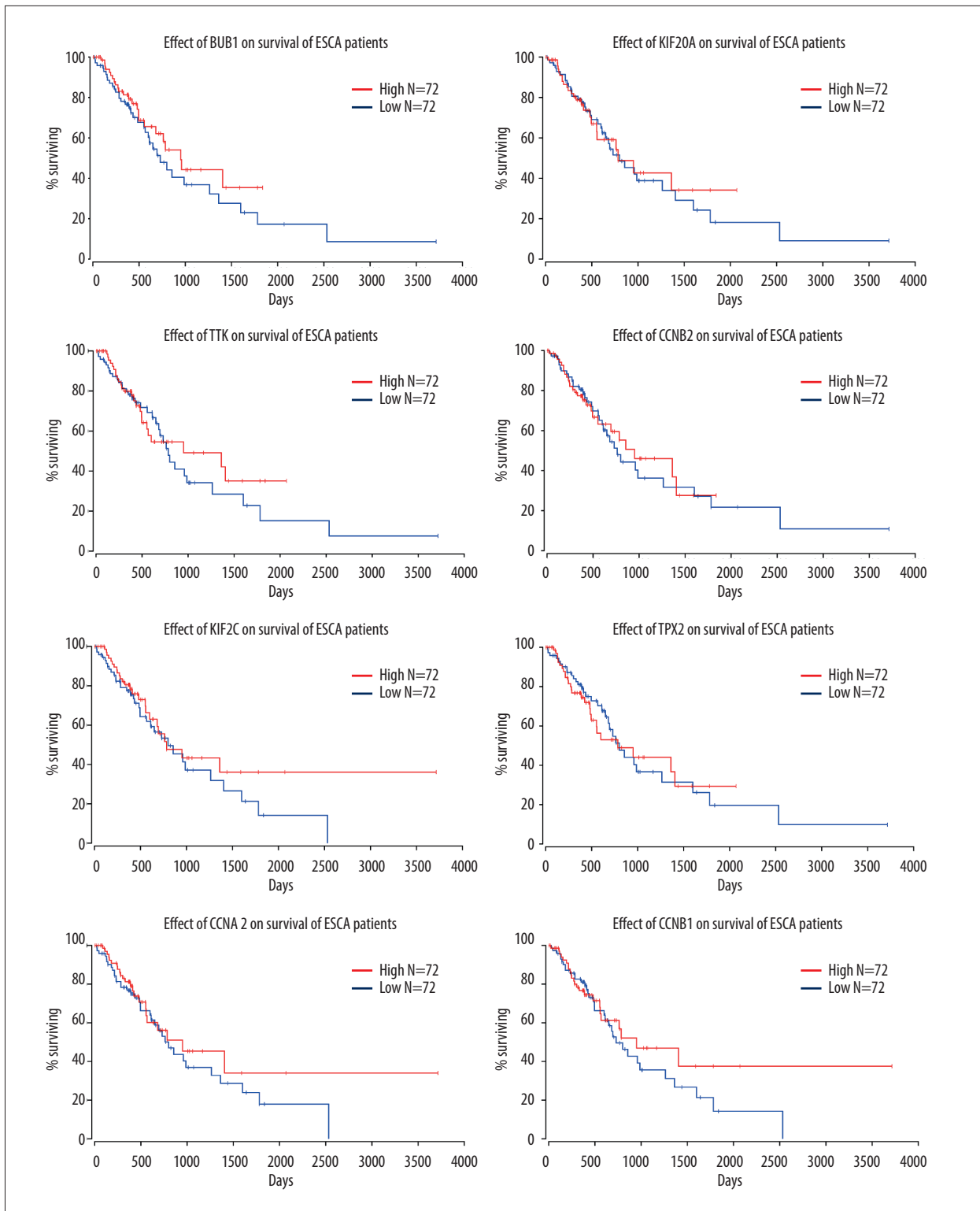


Figure 11. Effects of the top 10 hub genes on prognosis of ESCA patients, as calculated by OncoLnc. All of the hub genes improved late survival time of ESCA patients ($x > 2000$), while few exhibited any association with early survival time.

molecular functions. Even though we analyzed two microarray datasets containing data from patients diagnosed with ESCA, the chosen samples in our research are still inadequate for definitive conclusions, especially in light of the scarcity of experimental evidence related to our findings. It will be necessary to validate our research findings through practical experiments, such as immunohistochemistry on tumor tissue and paired healthy control tissue.

Conclusion

In this research, a total of 210 ESCA-related DEGs were found, and their enriched functions and pathways were analyzed using bioinformatics methods. Taking the mechanistic link between enriched pathways and ESCA into consideration, our results may provide helpful information for understanding ESCA pathology and ESCA treatment. The PPI network we constructed from the DEGs revealed that these genes mediate the occurrence and development of ESCA through multi-gene interactions. From these, we selected the top 10 hub genes: TOP2A

(highest ranking of degree), UBE2C, BUB1, KIF20A, TTK, CCNB2, KIF2C, TPX2, CCNA2, and CCNB1. These genes are closely associated with the etiology and prognosis of ESCA, and have potential as therapeutic or early-diagnostic biomarkers. Nevertheless, there are some limitations in our research. The absence of laboratory evidence imposes restrictions on the conclusions that can be drawn from our results. In addition, there were no more than 10 ESCA patients in each sample; this sample size may be insufficient. Therefore, in order to verify our findings, further experimental research, such as immunohistochemistry studies and large clinical studies, is needed.

Acknowledgements

We express our cordial thanks to all those who participated in this study.

Conflict of interest

None.

References:

1. Abnet CC, Arnold M, Wei WQ: Epidemiology of esophageal squamous cell carcinoma. *Gastroenterology*, 2018; 154(2): 360–73
2. Pennathur A, Gibson MK, Jobe BA et al: Oesophageal carcinoma. *Lancet*, 2013; 381(9864): 400–12
3. Smyth EC, Lagergren J, Fitzgerald RC et al: Oesophageal cancer. *Nat Rev Dis Primers*, 2017; 3: 17048
4. Sardana RK, Chhikara N, Tanwar B et al: Dietary impact on esophageal cancer in humans: A review. *Food Funct*, 2018; 9(4): 1967–77
5. Coleman HG, Xie SH, Lagergren J: The epidemiology of esophageal adenocarcinoma. *Gastroenterology*, 2018; 154(2): 390–405
6. Gharahkhani P, Fitzgerald RC, Vaughan TL et al: Genome-wide association studies in oesophageal adenocarcinoma and Barrett's oesophagus: A large-scale meta-analysis. *Lancet Oncol*, 2016; 17(10): 1363–73
7. Domper Arnal MJ, Ferrández Arenas Á, Lanás Arbeloa Á: Esophageal cancer: Risk factors, screening and endoscopic treatment in Western and Eastern countries. *World J Gastroenterol*, 2015; 21(26): 7933–43
8. Lagergren J, Smyth E, Cunningham D et al: Oesophageal cancer. *Lancet*, 2017; 390(10110): 2383–96
9. Alsop BR, Sharma P: Esophageal cancer. *Gastroenterol Clin North Am*, 2016; 45(3): 399–12
10. Wang C, Wang J, Chen Z et al: Immunohistochemical prognostic markers of esophageal squamous cell carcinoma: A systematic review. *Chin J Cancer*, 2017; 36(1): 65
11. Hernández M, Quijada NM, Rodríguez-Lázaro D et al: [Bioinformatics of next generation sequencing in clinical microbiology diagnosis]. *Rev Argent Microbiol*, 2019 [Online ahead of print]
12. Keerthikumar S: An introduction to proteome bioinformatics. *Methods Mol Biol*, 2017; 1549: 1–3
13. Peng D, Guo Y, Chen H et al: Integrated molecular analysis reveals complex interactions between genomic and epigenomic alterations in esophageal adenocarcinomas. *Sci Rep*, 2017; 7: 40729
14. He F, Ai B, Tian L: Identification of genes and pathways in esophageal adenocarcinoma using bioinformatics analysis. *Biomed Rep*, 2018; 9(4): 305–12
15. Ming XY, Zhang X, Cao TT et al: RHCG suppresses tumorigenicity and metastasis in esophageal squamous cell carcinoma via inhibiting NF- κ B Signaling and MMP1 expression. *Theranostics*, 2018; 8(1): 185–98
16. Liu D, Xu X, Wen J et al: Integrated genome-wide analysis of gene expression and DNA copy number variations highlights stem cell-related pathways in small cell esophageal carcinoma. *Stem Cells Int*, 2018; 2018: 3481783
17. Zhou Y, Zhou B, Pache L et al: Metascape provides a biologist-oriented resource for the analysis of systems-level datasets. *Nat Commun*, 2019; 10(1): 1523
18. Xie C, Mao X, Huang J et al: KOBAS 2.0: a web server for annotation and identification of enriched pathways and diseases. *Nucleic Acids Res*, 2011; 9: W316–22
19. Szklarczyk D, Gable AL, Lyon D et al: STRING v11: Protein-protein association networks with increased coverage, supporting functional discovery in genome-wide experimental datasets. *Nucleic Acids Res*, 2019; 47: D607–13
20. Shannon P, Markiel A, Ozier O et al: Cytoscape: A software environment for integrated models of biomolecular interaction networks. *Genome Res*, 2003; 13(11): 2498–504
21. Tang Z, Kang B, Li C, et al: GEPIA2: An enhanced web server for large-scale expression profiling and interactive analysis. *Nucleic Acids Res*, 2019; 47: W556–60
22. Anaya J: OncoLnc: Linking TCGA survival data to mRNAs, miRNAs, and lncRNAs. *Peer J Computer Science*, 2016; 2: e67
23. Canman JC, Cabernard C: Mechanics of cell division and cytokinesis. *Mol Biol Cell*, 2018; 29(6): 685–86
24. López-Lázaro M: The stem cell division theory of cancer. *Crit Rev Oncol Hematol*, 2018; 123: 95–113
25. Kar S: Unraveling cell-cycle dynamics in cancer. *Cell Syst*, 2016; 2(1): 8–10
26. Wen J, Hu Y, Liu Q et al: miR-424 coordinates multilayered regulation of cell cycle progression to promote esophageal squamous cell carcinoma cell proliferation. *EBioMedicine*, 2018; 37: 110–24
27. Lu Z, Ren Y, Zhang M et al: FLI-06 suppresses proliferation, induces apoptosis and cell cycle arrest by targeting LSD1 and Notch pathway in esophageal squamous cell carcinoma cells. *Biomed Pharmacother*, 2018; 107: 1370–76
28. Costa RLB, Han HS, Gradishar WJ: Targeting the PI3K/AKT/mTOR pathway in triple-negative breast cancer: a review. *Breast Cancer Res Treat*, 2018; 169(3): 397–406
29. Slattery ML, Mullany LE, Sakoda LC et al: The PI3K/AKT signaling pathway: Associations of miRNAs with dysregulated gene expression in colorectal cancer. *Mol Carcinog*, 2018; 57(2): 243–61

30. Wang SS, Chen YH, Chen N et al. Hydrogen sulfide promotes autophagy of hepatocellular carcinoma cells through the PI3K/Akt/mTOR signaling pathway. *Cell Death Dis*, 2017; 8(3): e2688
31. Li B, Xu WW, Lam AKY et al: Significance of PI3K/AKT signaling pathway in metastasis of esophageal squamous cell carcinoma and its potential as a target for anti-metastasis therapy. *Oncotarget*, 2017; 8(24): 38755–66
32. Wu N, Du Z, Zhu Y et al: The expression and prognostic impact of the PI3K/AKT/mTOR signaling pathway in advanced esophageal squamous cell carcinoma. *Technol Cancer Res Treat*, 2018; 17: 1533033818758772
33. Shi N, Yu H, Chen T: Inhibition of esophageal cancer growth through the suppression of PI3K/AKT/mTOR signaling pathway. *Onco Targets Ther*, 2019; 12: 7637–47
34. Zhu X, Li Z, Li T et al: Osthole inhibits the PI3K/AKT signaling pathway via activation of PTEN and induces cell cycle arrest and apoptosis in esophageal squamous cell carcinoma. *Biomed Pharmacother*, 2018; 102: 502–9
35. Li ZH, Cui D, Qiu CJ et al: Cyclic nucleotide signaling in sensory neuron hyperexcitability and chronic pain after nerve injury. *Neurobiol Pain*, 2019; 6: 100028
36. Spiller F, Oliveira Formiga R, Fernandes da Silva Coimbra J et al: Targeting nitric oxide as a key modulator of sepsis, arthritis and pain. *Nitric Oxide*, 2019; 89: 32–40
37. Inserte J, Garcia-Dorado D: The cGMP/PKG pathway as a common mediator of cardioprotection: translatability and mechanism. *Br J Pharmacol*, 2015; 172(8): 1996–2009
38. Tanțău M, Laszlo M, Tanțău A: Barrett's esophagus – state of the art. *Chirurgia (Bucur)*, 2018; 113(1): 46–60
39. Kim H, Kim YM: Pan-cancer analysis of somatic mutations and transcriptomes reveals common functional gene clusters shared by multiple cancer types. *Sci Rep*, 2018; 8(1): 6041
40. Wood DJ, Endicott JA: Structural insights into the functional diversity of the CDK-cyclin family. *Open Biol*, 2018; 8(9): 180112
41. Ma Q: MiR-219-5p suppresses cell proliferation and cell cycle progression in esophageal squamous cell carcinoma by targeting CCNA2. *Cell Mol Biol Lett*, 2019; 24: 4
42. Zeng R, Liu Y, Jiang ZJ et al: EPB41L3 is a potential tumor suppressor gene and prognostic indicator in esophageal squamous cell carcinoma. *Int J Oncol*, 2018; 52(5): 1443–54
43. Qian X, Song X, He Y et al: CCNB2 overexpression is a poor prognostic biomarker in Chinese NSCLC patients. *Biomed Pharmacother*, 2015; 74: 222–27
44. Li R, Jiang X, Zhang Y et al: Cyclin B2 overexpression in human hepatocellular carcinoma is associated with poor prognosis. *Arch Med Res*, 2019; 50(1): 10–17
45. Shi Q, Wang W, Jia Z et al: ISL1, a novel regulator of CCNB1, CCNB2 and c-MYC genes, promotes gastric cancer cell proliferation and tumor growth. *Oncotarget*, 2016; 7(24): 36489–500
46. Lucanus AJ, Yip GW: Kinesin superfamily: Roles in breast cancer, patient prognosis and therapeutics. *Oncogene*, 2018; 37(7): 833–38
47. Wu WD, Yu KW, Zhong N et al: Roles and mechanisms of Kinesin-6 KIF20A in spindle organization during cell division. *Eur J Cell Biol*, 2019; 98(2–4): 74–80
48. Gilbert SP, Guzik-Lendrum S, Rayment I: Kinesin-2 motors: Kinetics and biophysics. *J Biol Chem*, 2018; 293(12): 4510–18
49. Duan H, Zhang X, Wang FX et al: KIF-2C expression is correlated with poor prognosis of operable esophageal squamous cell carcinoma male patients. *Oncotarget*, 2016; 7(49): 80493–507
50. Bush NG, Evans-Roberts K, Maxwell A: DNA topoisomerases. *EcoSal Plus*, 2015; 6(2): 10
51. Purim O, Beny A, Inbar M et al: Biomarker-driven therapy in metastatic gastric and esophageal cancer: Real-life clinical experience. *Target Oncol*, 2018; 13(2): 217–26
52. Zhang S, Jiang H, Xu Z et al: The resistance of esophageal cancer cells to paclitaxel can be reduced by the knockdown of long noncoding RNA DDX11-AS1 through TAF1/TOP2A inhibition. *Am J Cancer Res*, 2019; 9(10): 2233–48
53. Raaijmakers JA, van Heesbeen RGHP, Blomen VA et al. BUB1 is essential for the viability of human cells in which the spindle assembly checkpoint is compromised. *Cell Rep*, 2018; 22(6): 1424–38
54. Doak SH, Jenkins GJ, Parry EM et al: Differential expression of the MAD2, BUB1 and HSP27 genes in Barrett's oesophagus-their association with aneuploidy and neoplastic progression. *Mutat Res*, 2004; 547(1-2): 133–44
55. Nicolau-Neto P, Palumbo A, De Martino M et al: UBE2C is a transcriptional target of the cell cycle regulator FOXM1. *Genes (Basel)*, 2018; 9(4): 188
56. Li L, Li X, Wang W et al: UBE2C is involved in the functions of ECRG4 on esophageal squamous cell carcinoma. *Biomed Pharmacother*, 2018; 98: 201–6
57. Pachis ST, Kops GJPL: Leader of the SAC: Molecular mechanisms of Mps1/TTK regulation in mitosis. *Open Biol*, 2018; 8(8): 180109
58. Mizukami Y, Kono K, Daigo Y et al: Detection of novel cancer-testis antigen-specific T-cell responses in TIL, regional lymph nodes, and PBL in patients with esophageal squamous cell carcinoma. *Cancer Sci*, 2008; 99(7): 1448–54
59. Iwahashi M, Katsuda M, Nakamori M et al: Vaccination with peptides derived from cancer-testis antigens in combination with CpG-7909 elicits strong specific CD8+ T cell response in patients with metastatic esophageal squamous cell carcinoma. *Cancer Sci*, 2010; 101(12): 2510–17
60. Sui C, Song Z, Yu H et al: Prognostic significance of TPX2 and NIBP in esophageal cancer. *Oncol Lett*, 2019; 18(4): 4221–29
61. Niu H, Gong L, Tian X et al: Low expression of miR-491 promotes esophageal cancer cell invasion by targeting TPX2. *Cell Physiol Biochem*, 2015; 36(6): 2263–73